Measurement of Pool Boiling Heat Transfer Coefficient with an Insulated Stainless-Steel Block

Viktor Vajc[1,*], and *Martin* Dostál[1]

[1]Department of Process Engineering, Faculty of Mechanical Engineering, Czech Technical University, 166 07 Prague, Czech Republic

Abstract. We have designed an apparatus dedicated for measurement of heat transfer coefficient during saturated nucleate pool boiling. After several performed measurements, we have applied three important modifications of the apparatus motivated by discrepancies between measured and correlated heat transfer coefficients. Firstly, the cubic stainless-steel heated block of the apparatus no longer accommodates heating cartridges. It now stands on a copper carrier of the cartridges, which are vertically oriented. Secondly, we have insulated the heated block with plates made of cellular glass. Thirdly, thermocouples used for measurement of temperatures inside the block have been fixated with a special high-temperature adhesive. These modifications were applied in order to improve the temperature distribution inside the block and to eliminate the impact of surroundings on measured heat transfer coefficients. This contribution presents and discusses experimental results obtained with these modifications.

1 Introduction

We have performed several experiments with our apparatus designed for measurement of heat transfer coefficient during saturated nucleate pool boiling. Obtained results are presented in our article [1], which was written for EFM 2018 conference. The results were compared with five verified correlations.

Eight experimentally found datapoints were published in [1]. Three of them evinced a strong discrepancy for heat flux slightly above 80 kW m^{-2}. Remaining five datapoints evinced a trend which was more or less comparable with trends of correlations, but obtained heat transfer coefficients were slightly higher than correlated values. These eight datapoints were obtained for a very small range of heat fluxes from around 80 up to 100 kW m^{-2}. This article presents and discusses a set of 58 datapoints obtained for heat fluxes from 20 up to 150 kW m^{-2}. Such a set is much more appropriate for making better-founded conclusions.

2 Correlations Used for Comparison

In order to verify our experimental results, we use five correlations briefly described in [1]: Rohsenow [2], Mostinski [3], Stephan and Abdelsalam [4], Nishikawa [5] and Yagov [6]. In this article, Forster and Zuber correlation [7] in the form taken from [8]

$$\alpha = \frac{0.00122\,\Delta T^{0.24}\,\Delta p^{0.75} c_{p,\mathrm{L}}^{0.45}\,\varrho_{\mathrm{L}}^{0.49}\,\lambda_{\mathrm{L}}^{0.79}}{\sigma^{0.5}\,\Delta h_{\mathrm{LG}}^{0.24}\,\mu_{\mathrm{L}}^{0.29}\,\varrho_{\mathrm{G}}^{0.24}} \tag{1}$$

is also included. However, correlation (1) is implicit, because superheat during saturated boiling

$$\Delta T = T_{\mathrm{w}} - T_{\mathrm{sat}} = q/\alpha \tag{2}$$

and difference of saturation pressures

$$\Delta p = p_{\mathrm{sat}}(T_{\mathrm{w}}) - p_{\mathrm{sat}}(T_{\mathrm{sat}})\,. \tag{3}$$

are both functions of heat transfer coefficient α. Therefore, we solved correlation (1) iteratively.

3 Experimental Apparatus

Our apparatus, see Fig. 1, is dedicated for measurement of heat transfer coefficient during saturated nucleate pool boiling under standard atmospheric pressure. It consists of stainless-steel bottom with a square cut. Stainless-steel block, see Fig. 2, is inserted through the cut. The gap between the bottom and the block is sealed with a combination of silicon *Ceresit CS 28* and epoxy *EPO-TEK 302-3M-R*. The block stands on a copper carrier of five vertically oriented heating cartridges, see Fig. 3. The carrier and the block are insulated with five plates made of cellular glass *Foamglas Perinsul S*. Top face of the block with dimensions of 48×48 mm is the wall on which boiling occurs. Temperature field inside the block is measured with six sheathed thermocouples *Omega GKMQSS-M100U-150* accommodated inside six holes (D = 1 mm, L = 24 mm) drilled into the block. These holes were filled with alumina-based adhesive *Aremco Ceramabond 670*. Adhesives and other

*e-mail: viktor.vajc@fs.cvut.cz

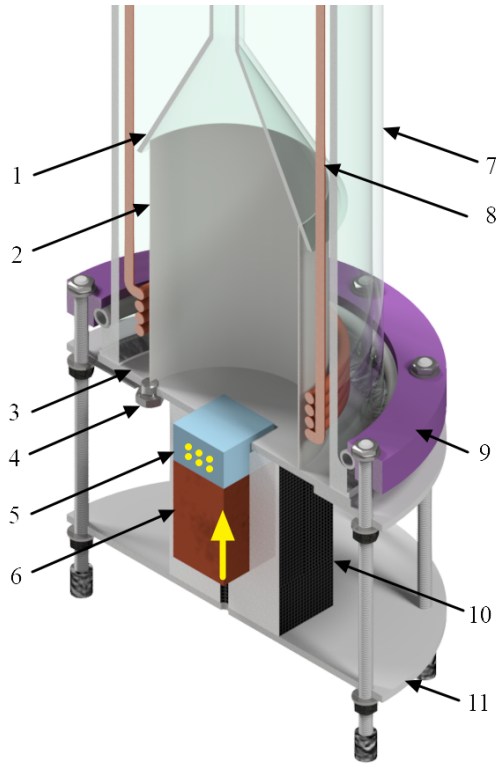

Fig. 1. Experimental apparatus: 1 Funnel roof, 2 Separating tube, 3 Bottom, 4 Plug, 5 Heated stainless-steel block, 6 Copper carrier of heating cartridges, 7 Glass cylinder, 8 Auxiliary heater, 9 Flange, 10 Thermal insulation, 11 Assembly flange. Six holes for thermocouples and orientation of heating cartridges inside the carrier are marked with yellow color.

methods for attachment of thermocouples to the block are discussed in [9].

On the bottom stands a glass cylinder with inner diameter of 200 mm and length of 500 mm. PTFE gasket is placed between the bottom and the cylinder. The cylinder is opened to the surroundings and serves as a reservoir for the boiling liquid. Temperature of the boiling liquid is measured with thermocouple probes *Omega TJ2-CPSS-M15U-600*. Auxiliary heating spiral is inserted into the cylinder from its top. Power to the heating cartridges and to the heating spiral is supplied and regulated with variacs. Inside the cylinder, on the bottom stands a stainless-steel tube (D = 70 mm, L = 200 mm). Glass funnel was placed on the top of the tube.

Cold junctions of all thermocouples were placed into calibration reference chamber *Omega TRCIII-A* via cold-junction probes *Omega TRP-K-36* and *Omega TRP-T-36*. DAQ module *JanasCard AD24USB* provided A/D conversion between thermocouples and PC.

4 Modifications of the Apparatus

The current experimental apparatus in Fig. 1 was developed from an older version of the apparatus described in [1]. In this section, we mention major modifications and justification for them.

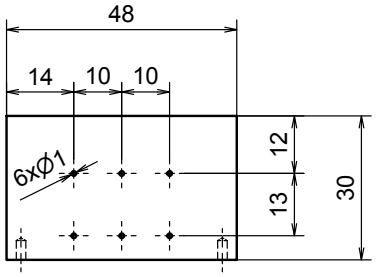

Fig. 2. Heated block.

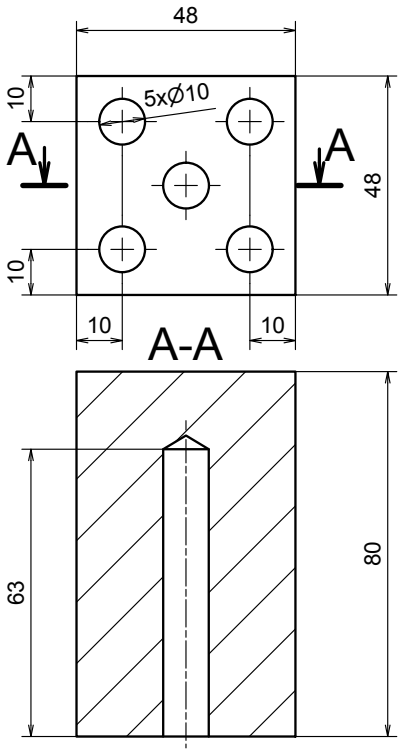

Fig. 3. Carrier of heating cartridges.

4.1 Elimination of Subcooling

In [1], we have mentioned that we were unable to achieve saturated boiling. Furthemore, temperature of the boiling liquid was not stable when we heated the boiling liquid only with primary cartridge heaters. Therefore, we installed secondary auxiliary heater. Boiling was, however, still subcooled in average by 0.6 °C for datapoints presented in [1]. Because of the subcooling, we were forced to perform experiments only for heat fluxes higher than 80 kW m^{-2}. For lower heat fluxes, the subcooling would have been at least several degrees Celsius. We tried to eliminate this subcooling using insulation of glass cylinder made of glass wool, but the situation did not improve.

After that, we tried to separate and enclose the space above the heating wall. For that, we used a stainless-steel tube, see part no. 2 in Fig. 1, and on the top of the tube we placed a funnel roof, see part no. 1 in Fig. 1. This modification completely eliminated the subcooling. Moreover, we were able to remove insulation from the glass cylinder. Now, we are able to reach saturated boiling for heat fluxes higher than approximately 25 kW m^{-2}. For lower heat fluxes, subcooling of several tenths of °C emerges.

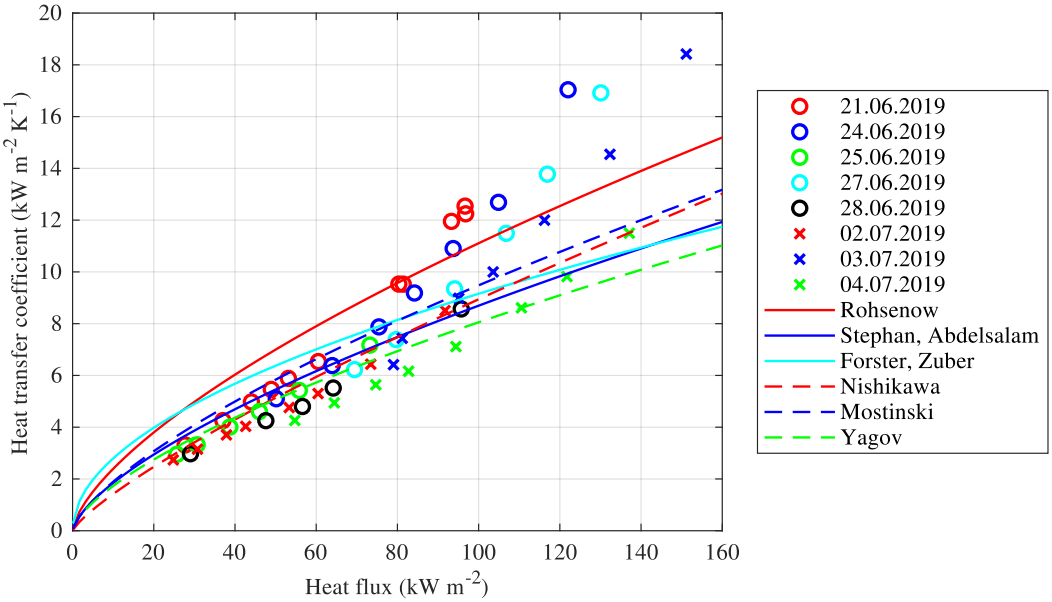

Fig. 4. Results of experimental measurements.

Another positive effect of the funnel roof and stainless-steel tube is that boiling above the heating surface is no longer affected by boiling on the auxiliary heater.

4.2 Thermal Insulation for Heated Block

In the past, we insulated the heated block with glass wool. The disadvantage of glass wool is its pliability which made the installation complicated. Another disadvantage is that glass wool is not suitable into wet environments (and the environment is wet in our case as the apparatus in Fig. 1 is opened to surroundings). Therefore, we did a literary review in order to find a suitable insulation material.

Literature very often mentions insulations made of polymers (PTFE, PEEK, PI, Teflon, Nylon, etc.), wools (fiberglass, mineral, rock, kaolin and other wools) and ceramic in the form of tablets, blankets made of ceramic fibers or custom-made parts. Combined insulation composed from several layers made of these materials is also often used. However, none of these materials seemed to be suitable for our application. Therefore, we had chosen not to follow the literature and used insulation made of cellular glass *Foamglas Perinsul S*, see part no. 10 in Fig. 1. The main advantages of this insulation are that its thermal conductivity is lower than 0.05 W m^{-1} K^{-1}, maximum operational temperature is 430 °C and that the material is water-resistant and impermeable for vapor.

4.3 Two-Piece Heated Block

Since the beginning of our experiments, we have observed horizontal temperature differences inside the heated block. These differences were strongly dependent on axial position of heating cartridges inside holes. In [1], the block was made of a single stainless-steel piece. In order to decrease the differences, we split the block into a copper carrier, see Fig. 3, and the block itself, see Fig. 2. The carrier accommodates five vertically oriented heating cartridges (we used three horizontally oriented cartridges in [1]). Vertical orientation enables us to insulate the carrier and the block more easily. Five holes for these cartridges (D = 10 mm, L = 63 mm) were precisely manufactured in order to reduce the contact thermal resistances between cartridges and the carrier as much as possible. Copper was chosen in order to provide an uniform distribution of temperature and heat flux. We are, of course, fully aware that we created another contact resistance between the carrier and the block by splitting the single-piece block originally used in [1] into two pieces. However, we believe that the contact resistances between cartridges and the carrier are more important with respect to the temperature field inside the block. Moreover, when we want to switch the heated block for another piece, we will not have to deal with precise manufacturing of holes for heating cartridges again.

4.4 Thermocouples

Heat transfer coefficients measured with our apparatus are strongly dependent on temperatures measured inside the heated block. From our experience, even a slight change of position of a thermocouple, which is accommodated inside the heated block, has a strong impact on measured temperature. Therefore, we tried to fixate our thermocouples with a suitable agent.

In article [9], we did another literary review and found out that three methods are commonly used for attachment of thermocouples in pool boiling apparatuses: peening or crimping, melting and fixation with an adhesive. We have chosen to use an adhesive for our *Omega GKMQSS-M100U-150* thermocouples. However, the most often used adhesives such as epoxies or cyanoacrylate-based glues are not acceptable for our case, because their operational temperature is at most 250 °C. Yet, sometimes, we measured temperatures around 360 °C for the lower line of thermocouples. Therefore, we have chosen an alumina-based adhesive *Aremco Ceramabond 670* with maximum

Table 1. Analysis of influence of horizontal temperature difference of ±1 °C on resulting values for three different datapoints.

Case	ΔT_{up} (°C)	ΔT_{lo} (°C)	T_{up} (°C)	T_{lo} (°C)	T_w (°C)	q (kW m^{-2})	α_i (kW m^{-2} K^{-1})	α_i/α_0 (–)	$\alpha_i - \alpha_0$ (kW m^{-2} K^{-1})
0	0.0	0.0	137.6	169.7	108.0	37.0	4.2	1.000	0.0
1	+1.0	+1.0	138.6	170.7	109.0	37.0	3.8	0.898	−0.4
2	−1.0	−1.0	136.6	168.7	107.0	37.0	4.8	1.129	+0.5
3	+1.0	−1.0	138.6	168.7	110.8	34.7	3.0	0.708	−1.2
4	−1.0	+1.0	136.6	170.7	105.1	39.3	6.6	1.573	+2.4
0	0.0	0.0	172.8	243.3	107.6	81.4	9.7	1.000	0.0
1	+1.0	+1.0	173.8	244.3	108.6	81.4	8.7	0.894	−1.0
2	−1.0	−1.0	171.8	242.3	106.6	81.4	11.0	1.135	+1.3
3	+1.0	−1.0	173.8	242.3	110.5	79.1	7.0	0.726	−2.7
4	−1.0	+1.0	171.8	244.3	104.8	83.7	15.1	1.554	+5.4
0	0.0	0.0	181.7	262.6	107.1	93.3	11.8	1.000	0.0
1	+1.0	+1.0	182.7	263.6	108.1	93.3	10.5	0.888	−1.3
2	−1.0	−1.0	180.7	261.6	106.1	93.3	13.5	1.145	+1.7
3	+1.0	−1.0	182.7	261.6	109.9	91.0	8.5	0.717	−3.3
4	−1.0	+1.0	180.7	263.6	104.3	95.6	18.9	1.602	+7.1

operational temperature of 1 650 °C and dynamic viscosity of 5 Pa s.

The adhesive should have eliminated the unwanted change of position of thermocouple-junctions inside the holes during our experiments. Furthermore, it should have reduced contact thermal resistances between thermocouple-junctions and the heated block in order to reduce the horizontal temperature differences mentioned in section 4.3. While the first objective was accomplished, the second was not. More details are given in section 5.

4.5 Minor Modifications

In [1], we mentioned that we had observed limescale deposits on the heating wall. In this article, all experiments were performed with water demineralized with unit *Aqual 29 XL*.

In [1], we have used ordinary epoxy *Kittfort 1200* together with high-temperature silicone *Versachem Mega Copper*. This combination evinced noticeable degradation after each experiment and has to be reapplied after several conducted experiments. Because of that, we switched it for low-viscous epoxy *EPO-TEK 302-3M-R* and high-temperature silicone *Ceresit CS 28*. This combination has long-term temperature durability up to 260 °C. We were able to obtain all datapoints presented in this article with a single application of the silicone and the epoxy.

5 Experimental Measurements

This section presents results of eight experimental runs with 58 obtained datapoints. All of the datapoints were obtained after reaching steady-state boiling of demineralized water under atmospheric pressure.

5.1 Results

Results of our experimental measurements can be seen in Fig. 4. We can distinguish between two regions in Fig. 4:

1. For heat fluxes lower than approximately 90 kW m^{-2}, measured heat transfer coefficients seems to be slightly lower than correlated values. Also, there seems to be a trend of modest (although not monotone) decrease of heat transfer coefficient with time.
2. For heat fluxes higher than approximately 90 kW m^{-2}, measured heat transfer coefficients outreach correlated values by a significant amount. The discrepancy between measured and correlated values increase with increased heat flux. The decreasing trend of heat transfer coefficient with time seems to be pronounced for these heat fluxes.

From Fig. 4, we can observe that the trend of increased heat transfer coefficients for heat fluxes higher than 90 kW m^{-2} is noticeable for all performed experiments. Also, the trend is reproducible within each measurement, as is obvious from two points obtained on 21 June for heat fluxes of about 80 kW m^{-2} and three points obtained on the same day for heat fluxes slightly below 100 kW m^{-2}.

5.2 Discussion

In article [1], we mention that we have observed unwanted horizontal temperature differences inside the heated block manufactured from single stainless-steel piece. According to the article, the differences were from about 3 up to 4 °C for the upper line and from about 6 up to 8 °C for the lower line of thermocouples. In order to reduce these differences, we modified the apparatus according to section 4. However, we have to admit that implemented modifications did not eliminate these differences. For measurements presented in Fig. 4, we observed horizontal differences of about 10 °C in the lower line and of about 2 °C in the upper line of thermocouples. However, these differences were dependent on heat flux and tended to increase with increased heat flux flowing through the heated block.

We currently believe that the differences are caused by these thermal resistances:

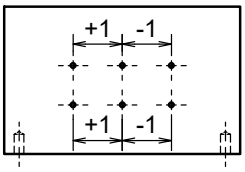

Fig. 5. Symmetrical temperature differences.

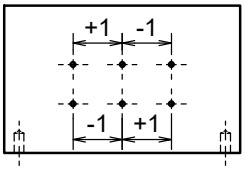

Fig. 6. Crossed temperature differences.

1. Contact resistances between cartridge heaters and the copper carrier
2. Contact resistances between thermocouples and stainless-steel block
3. Contact resistance between the carrier and the block

We also believe that the differences might be responsible for the observed and unexpected trend in Fig. 4. It is certain that horizontal temperature differences have a strong impact on measured heat transfer coefficients.

6 Analysis of Horizontal Differences

In order to understand the impact of temperature differences on resulting values, we analyze effect of artificially induced difference of 1 °C on resulting values in this section. Let us assume, that the temperature of the upper central thermocouple is 172.8 °C, temperature of the lower central thermocouple is 243.3 °C and that water boils at 99.2 °C (these are average temperatures[1] taken from one datapoint measured on 21 June). From these temperatures we can calculate[2] heat flux of 81.4 kW m^{-2} and heat transfer coefficient of 9.7 kW m^{-2} K^{-1}. Now, we fix temperature of the boiling liquid at 99.2 °C and suppose four different cases:

Case 1: There are temperature differences of +1 °C for both thermocouples on the left. That means that for the left side the upper thermocouple measures 173.8 °C and lower thermocouple 244.3 °C. Form these temperatures, we obtain heat flux 81.4 kW m^{-2} and heat transfer coefficient 8.7 kW m^{-2} K^{-1}.

Case 2: There are temperature differences of −1 °C for both thermocouples on the right. For the upper right thermocouple, we then get 171.8 °C and for lower right thermocouple 242.3 °C. Heat flux is then 81.4 kW m^{-2} and heat transfer coefficient 11.0 kW m^{-2} K^{-1}.

Case 3: There is a temperature difference of +1 °C for the upper and −1 °C for the lower thermocouple on the left. This gives us upper temperature of 173.8 °C and lower temperature of 242.3 °C, heat flux of 79.1 kW m^{-2} and heat transfer coefficient 7.0 kW m^{-2} K^{-1}.

Case 4: There is a temperature difference of −1 °C for the upper and +1 °C for the lower thermocouple on the right. Upper temperature is then 171.8 °C, lower temperature 244.3 °C, heat flux 83.7 kW m^{-2} and heat transfer coefficient 15.1 kW m^{-2} K^{-1}.

Results for all cases were put into Tab. 1 together with two other datapoints obtained on 21 June. *Case 0* in Tab. 1 are reference values without any imposed differences. One can make several observations from Tab. 1:

- Equal imposed differences do not affect the heat flux, but heat transfer coefficient is affected due to a change in extrapolated wall temperature T_w.
- When we impose temperature differences of opposite signs, there is a higher difference between resulting heat transfer coefficient α_i and original heat transfer coefficient α_0 compared to differences with the same sign. This difference of heat transfer coefficients unfolds for datapoints obtained under higher heat fluxes.
- Relative fractions of α_i/α_0 are mutually comparable for corresponding temperature differences across all three considered datapoints. However, for datapoints obtained under higher heat fluxes, α_0 is higher. Due to that, the difference in heat transfer coefficients $\alpha_i - \alpha_0$ is higher for these datapoints.

Table 2. Arithmetic means $\bar{\alpha}$ and maximum absolute deviations Δ calculated for datapoints from Tab. 1.

Distribution Fig. 5 and Fig. 6	$\bar{\alpha}$ (kW m^{-2} K^{-1})	Δ (kW m^{-2} K^{-1})
symmetrical	4.3	0.5
crossed	4.6	2.0
symmetrical	9.8	1.2
crossed	10.6	4.4
symmetrical	11.9	1.6
crossed	13.1	5.9

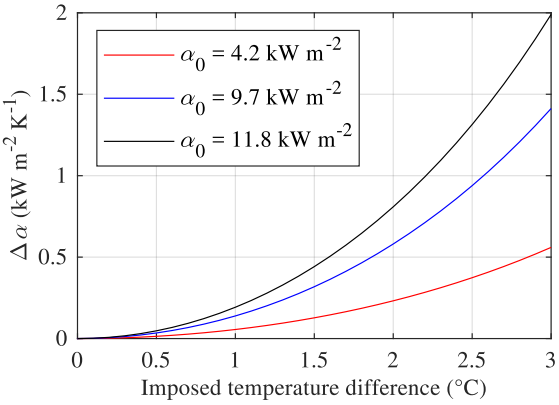

Fig. 7. Maximum absolute deviations of heat transfer coefficients between side and central rows of thermocouples for symmetrical temperature differences.

[1] We do not directly take temperatures measured with thermocouples in the central row, because they might be influenced by temperature differences as well.

[2] We suppose that thermal conductivity of the stainless steel is 15 W m^{-1} K^{-1} and that the heated block block has dimensions drawn in Fig. 2.

- As the extrapolated wall temperature T_w gets closer to the temperature of the boiling liquid T_L, the effect of temperature differences on resulting heat transfer coefficient gets more and more severe.

Let us consider two possible distributions of temperature differences inside the heated block. Fig. 5 shows symmetrical distribution, which is a combination of *Case 1* and *Case 2*. On the other hand, Fig. 6 shows crossed distribution, which is combined from *Case 3* and *Case 4*. From previous considerations, one can conclude that the symmetrically distributed differences should have lower impact on resulting values. To support this conclusion, Tab. 2 presents arithmetic means of heat transfer coefficient $\bar{\alpha}$ and maximum absolute deviations

$$\Delta = \max |\alpha_i - \bar{\alpha}| \ , \tag{4}$$

where i is an integer number and goes from 0 up to 4.

From Tab. 2, it is immediately clear that symmetrically imposed temperature differences results in lower Δ. From Tab. 1 and Tab. 2, it is also noticeable that values of heat transfer coefficient measured above the central row of thermocouples lies very close to the arithmetic mean for symmetrically imposed differences. However, it is a coincidence which occurs due to the fact that imposed differences were small. In order to prove that, Fig. 7 shows value of

$$\Delta\alpha = \frac{\alpha_1 + \alpha_2}{2} - \alpha_0 \tag{5}$$

as a function of imposed temperature difference for symmetrical temperature differences. The fraction in (5) is the arithmetic mean of heat transfer coefficients above the side rows of thermocouples and α_0 is heat transfer coefficient above the central row of thermocouples (without any imposed differences). From Fig. 7, it is obvious that the difference $\Delta\alpha$ non-linearly increases for higher imposed temperature differences for all investigated heat fluxes.

For crossed temperature differences, the situation is quite different compared with symmetrical differences. Arithmetic means $\bar{\alpha}$ are considerably shifted from values calculated above the central row of thermocouples and maximum deviations Δ are significantly higher, as can be seen in Tab. 2.

7 Conclusion

This article discusses modifications of experimental apparatus designed for measurement of heat transfer coefficient during saturated nucleate pool boiling. It presents experimental results obtained with these modifications and mentions problematic horizontal temperature differences which need to be eliminated or at least significantly lowered in order to achieve valuable experimental results. Analysis of effect of artificially induced temperature differences on resulting values is given. The analysis implies that symmetrical temperature differences inside the heated block affect the measurements to a much lower extent compared to crossed non-symmetrical temperature differences.

Our closest plan with the apparatus is to lower the horizontal temperature differences by reducing the contact thermal resistance between the carrier and the block. We want to bolt both parts together. We also intend to use a special graphite sheet as a thermal interface material.

This work was supported by the Ministry of Education, Youth and Sports of the Czech Republic under OP RDE grant number CZ.02.1.01/0.0/0.0/16_019/0000753 “Research centre for low-carbon energy technologies” and by the Grant Agency of the Czech Technical University in Prague, grant number SGS18/129/OHK2/2T/12.

Nomenclature

c_p	isobaric specific heat capacity	($J\,kg^{-1}\,K^{-1}$)
D	diameter	(m)
L	length	(m)
p	pressure	(Pa)
T	temperature	(°C)
α	heat transfer coefficient	($W\,m^{-2}\,K^{-1}$)
Δ	maximum absolute deviation	
Δh_{LG}	specific latent heat of vaporization	($J\,kg^{-1}$)
ΔT	superheat	(°C)
$\Delta\alpha$	difference of α defined in (5)	($W\,m^{-2}\,K^{-1}$)
λ	thermal conductivity	($W\,m^{-1}\,K^{-1}$)
μ	dynamic viscosity	(Pa s)
ϱ	density	($kg\,m^{-3}$)
σ	surface tension	($N\,m^{-1}$)

Subscripts:

0	reference value
G	related to vapor phase
i	ordinal index
L	related to liquid phase
lo	lower
sat	at saturation state
up	upper
w	related to the heating wall

References

1. V. Vajc, M. Dostál, EPJ Web of Conferences **213** (2019)
2. W.M. Rohsenow, Tech. rep., Div. of Industr. Coop., Heat Transf. Lab., Cambridge, MASS, USA (1952)
3. I.L. Mostkinski, Teploenergetika **10**, 66 (1963)
4. K. Stephan, M. Abdelsalam, Int. J. of Heat Mass Transf. **23**, 73 (1980)
5. K. Nishikawa, Y. Fujita, H. Ohta, S. Hidaka, Proc. 7th Int. Heat Transf. Conf. **4**, 61 (1982)
6. V.V. Yagov, Heat Mass Transf. **45**, 881 (2009)
7. H.K. Forster, N. Zuber, AIChE Journal **1**, 531 (1955)
8. G.F. Hewitt, in *Handbook of Heat Transfer* (McGraw-Hill, New York, NY, USA, 1998), pp. 989–1156, 3rd edn., ISBN 0-07-053555-8
9. V. Vajc, M. Dostál, Proc. 14th Int. Conf. on Heat Transf., Fluid Mech. and Thermodyn., pp. 808–813 (2019)